Properties of Isolated Recombinant N and C Domains of Chicken Troponin C†

Monica X. Li,‡ Murali Chandra,‡ Joyce R. Pearlstone,‡ Kathleen I. Racher,§ Genny Trigo-Gonzalez,§ Thor Borgford,§ Cyril M. Kay,‡ and Lawrence B. Smillie*,‡

MRC Group in Protein Structure and Function, Department of Biochemistry, University of Alberta, Edmonton, Alberta, Canada T6G 2H7, and Department of Chemistry and Institute of Molecular Biology and Biochemistry, Simon Fraser University, Burnaby, British Columbia, Canada V5A 1S6

Received September 7, 1993; Revised Manuscript Received November 8, 1993⊛

ABSTRACT: The two globular N and C domains of chicken troponin C (TnC) are connected by an exposed α-helix (designated D/E; residues 86–94). Recombinant N (residues 1–90) and C (residues 88–162) domains containing either F29 or W29 and F105 or W105 have been engineered and expressed in *Escherichia coli*. These termination and initiation sites were chosen to minimize disruption of side-chain interactions between the D/E helix and other residues. W29 and W105 served as useful spectral probes for monitoring Ca^{2+}-induced structural transitions of the N and C domains, respectively [Pearlstone et al. (1992) *Biochemistry 31*, 6545–6553; Trigo-Gonzalez et al. (1992) *Biochemistry 31*, 7009–7015]. By all criteria tested, the properties of the isolated F29W/N domain (1–90) were identical to those of the N domain in intact F29W. These included fluorescence emission spectra in the absence and presence of Ca^{2+}/Mg^{2+}, far-UV CD spectra, and Ca^{2+} affinity as monitored by fluorescence and ellipticity at 221 nm. Similar but not identical properties were observed for isolated F105W/C domain (88–162) and intact F105W. A summation of the far-UV CD spectra ($\pm Ca^{2+}$) of the two domains was virtually superimposable on that of the intact protein. Of the total Ca^{2+}-induced ellipticity change at 221 nm, 27% could be assigned to the N domain and 73% to the C domain. The data suggest a significant Ca^{2+}-induced transition involving secondary structural elements of the N domain. Similar but not identical Ca^{2+}-induced changes were observed in a truncated form of the N domain (F29W/N domain, 12–87) corresponding to the TR1C fragment (residues 9–84) of rabbit skeletal TnC.

As the Ca^{2+} binding member of the troponin complex, troponin C (TnC)[1] plays a key role in the Ca^{2+} regulation of contraction and relaxation in skeletal and cardiac muscles. Conformational changes in TnC induced by Ca^{2+} binding and dissociation are believed to be transmitted through the other members of the troponin complex, troponins I and T, to tropomyosin–actin, resulting in activation/inhibition of actomyosin ATPase and contraction/relaxation [for reviews, see Potter and Johnson (1982), Leavis and Gergely (1984), Grand (1985), Zot and Potter (1987), Parmacek and Leiden (1991), and Grabarek et al. (1992)].

Examination of the known crystal structure of TnC reveals a dumbbell-shaped molecule with two domains, N and C, connected through an extended helix, a portion of which is exposed to solvent and whose side chains show no interaction with those of the more globular N and C domains [for a review, see Strynadka and James (1989)]. Each domain contains two divalent metal binding sites, designated sites I and II in the N domain and sites III and IV in the C domain, each site consisting of the loop–helix–loop motif typical of this class of proteins. Sites III and IV are of relatively high affinity for Ca^{2+} ($K_a \cong 10^7$ M^{-1}) and also bind Mg^{2+} ($K_a \cong 10^3$ M^{-1}). Sites I and II are of lower affinity ($K_a \cong 10^5$–10^6 M^{-1}) and are believed to be specific for Ca^{2+}. Current evidence indicates a largely structural role for the C domain whose sites would be occupied by Ca^{2+}/Mg^{2+} throughout the contraction/relaxation cycle. The regulatory role is considered to be associated with the conformational changes induced by the binding and release of Ca^{2+} from N-domain sites I/II.

In the known X-ray structure of TnC, based on crystals grown at pH ≅5, sites I and II are empty whereas sites III and IV are occupied by Ca^{2+}. We refer to this known structure as the $2Ca^{2+}$ state. A hypothetical model for the $4Ca^{2+}$ state has been proposed by Herzberg et al. (1986) based on the extensive sequence similarity between the N and C domains. This transition from $2Ca^{2+}$ to $4Ca^{2+}$ states would involve a rearrangement of secondary structural elements such that helices B and C move as a unit relative to N, A, and D helices. The model predicts no change in the α-helical content of the molecule.

Elucidation of the X-ray structure of the $2Ca^{2+}$ state has raised a number of questions which several recent studies have been designed to address. These include among others: the relevance of the ~pH 5.0 crystal structure to that in solution at pH 7.0; the validity of the postulated Ca^{2+}-induced structural transition to the $4Ca^{2+}$ state; and the absence or presence of interdomain communication as it affects the properties of TnC alone or in complex with the other troponin components [for a recent review, see Grabarek et al. (1992)]. Much useful information bearing on these and other questions has been obtained from the properties of TnC fragments derived from either proteolytic or chemical cleavage. Of those available, the two tryptic fragments TR1C (residues 9–84) and TR2C (resides 89–159) correspond most closely to the N and C domains, respectively, although TR1C lacks residues 1–8, which make up the major portion of the N helix. While both fragments were reported to retain their original Ca^{2+} binding

† This study was supported by the Medical Research Council of Canada and the British Columbia Health Research Foundation. M.X.L., K.I.R., and T.B. were recipients of an Alberta Heritage Foundation for Medical Research Postdoctoral Fellowship, a Medical Research Council of Canada Studentship, and a British Columbia Research Scholarship Award, respectively.

‡ University of Alberta.

§ Simon Fraser University.

⊛ Abstract published in *Advance ACS Abstracts*, January 1, 1994.

[1] Abbreviations: TnC, troponin C; rTnC, recombinant troponin C.

0006-2960/94/0433-917$04.50/0 © 1994 American Chemical Society

properties, an absence of Ca^{2+}-induced structural changes as monitored by fluorescence and circular dichroism was described in the case of TR1C. As noted by Grabarek et al. (1992), the properties of these fragments indicated that there was little interaction between the two domains in intact TnC.

Other studies have indicated some degree of interdomain communication in intact TnC. In large part these have involved the measurement of spectral features arising from large aromatic probes covalently linked to either Met-25 (N domain) or Cys-98 (C domain) in rabbit TnC. Since the introduction of such probes may perturb the protein structure as well as its conformational transitions, observations based on their spectral features must be interpreted with caution.

In recent reports (Pearlstone et al., 1992; Trigo-Gonzalez et al., 1992), we have described two TnC mutants, F29W and F105W, which serve as useful spectral probes for monitoring specifically the Ca^{2+}- or Mg^{2+}-induced structural transitions of N and C domains, respectively, in the intact molecule. In the present work, we report the application of these probes to a comparison of the properties of isolated N (residues 1–90) and C (residues 88–162) domains with those of the intact molecule. Initiation and termination sites were chosen to minimize disruption of side-chain interactions of the D/E helix and adjacent domains. By all criteria examined, the properties of the N domain were found to be identical to those in the intact molecule. Those of the isolated C domain were dound to be slightly modified from those in the whole TnC. Of the total Ca^{2+}-induced ellipticity change at 221 nm for intact TnC, ~27% could be attributed to N domain (1–90), indicating a substantial secondary structural change. We have also prepared a truncated N domain (residues 12–87; chicken sequence numbering) lacking the N helix and corresponding to rabbit TnC fragment TR1C (residues 9–84). Contrary to earlier reports, we observe a significant Ca^{2+}-induced structural transition as monitored by circular dichroism and fluorescence which is similar but not identical to that attributable to isolated N domain (1–90) and to that in intact TnC.

EXPERIMENTAL PROCEDURES

Nomenclature of Proteins and Mutants. The sequence of chicken recombinant troponin C (rTnC) differs at two positions from the naturally occurring skeletal muscle protein (Golosinska et al., 1991). Thr-130 is substituted by Ile, and the N-terminal blocking acetyl group is replaced by Met. The chicken protein (residues 1–162) is extended by three residues at the NH_2-terminal end when compared with rabbit fast skeletal muscle TnC (residues 1–159). The numbering scheme used below is for the chicken TnC except as indicated. The designation N domain (1–90) is for the fragment encompassing residues 1–90 of rTnC. F29W/N domain (1–90) describes the same fragment in which F29 is mutated to W. Like intact rTnC, both of these preparations have an N-terminal Met in addition to residues 1–90. F29W/N domain (12–87) refers to the truncated fragment and corresponds closely to the TR1C tryptic fragment (residues 9–84) of rabbit fast muscle TnC (Leavis et al., 1978; Grabarek et al., 1981). Protein sequencing of the purified product shows that the initiation Met is cleaved off during expression in *Escherichia coli*. The nomenclature of C domain (88–162) and F105W/C domain (88–162) is similar to the above. Neither has an N-terminal Met since they were prepared by factor Xa cleavage of the expressed fusion proteins.

Construction of TnC Mutants and Protein Isolation. For the preparation of N domain (1–90) and F29W/N domain (1–90), the *Eco*RI DNA fragment (1.2 kb) containing the TnC gene was isolated from pLcIIFx.TnC (Reinach & Karlsson, 1988) and subcloned into pTZ18 plasmid DNA (Mead et al., 1986) to give pTZ18.TnC. The codon at position 91 in TnC was changed to a stop codon by performing site-specific mutagenesis using pTZ18.TnC single-stranded DNA containing uracil residues as the template DNA (Kunkel et al., 1987). The mutation was directed by the 17-base oligonucleotide 5′-AGGACGCCTAGGGCAAG-3′ where the underlined nucleotides correspond to codon 91. The entire region of the TnC gene was sequenced to ensure the validity of the mutant. The 1.2-kb *Eco*RI fragment was then ligated into the *Eco*RI sites of the expression vector pLcIIFx.TnC.

The double mutant carrying W at position 29 and a stop codon at position 91 was isolated as follows. The double-stranded DNA of pTZ18.TnC (91 stop) was cleaved with restriction endonucleases *Bst*XI and *Sal*I for which there are unique sites. The fragment resulting from this digest contained the coding region of TnC from codon 41 to the 3′ end of the TnC gene. This fragment was ligated into the *Bst*XI–*Sal*I fragment of pLcIIFx.TnC.F29W (Pearlstone at al., 1992).

For the preparation of C domain (88–162) and F105W/C domain (88–162), site-directed mutagenesis was performed by the olignucleotide-directed method as described for double priming (Carter et al., 1985). Two modified rTnC genes (cloned into the *Eco*RI site of M13mp19) containing either the substitution F29W or the substitution F105W (Pearlstone et al., 1992; Trigo-Gonzalez et al., 1992) were used as templates. The oligonucleotide used to direct the deletion of the first 87 amino acid residues was 5′-TCGAGGGTAGG-**GA**GGACGCCAA-3′ where the factor Xa cleavage site at the 5′ end of the TnC gene is underlined and the codon for amino acid residue 88 is in boldface letters. Single-stranded phage containing the mutation were identified by dideoxynucleotide sequencing. The C domain (88–162) and F105W/C domain (88–162) mutant gene fragments were purified from replicative form M13 after digestion with *Eco*RI and subcloned into the vector pLcIIFx.TnC (Reinach & Karlsson, 1988) which had been cut with *Eco*RI and treated with calf intestinal phosphatase.

Each of the pLcIIFx constructs prepared as described above was transformed into the *E. coli* strain QY13. The resulting transformants were tested for expression of the fusion proteins. Plasmid DNA from expressing clones was purified, and the mutated TnC genes were sequenced. Large-scale expression of the fusion proteins and their purification and cleavage with factor Xa were as described previously (Golosinska et al., 1991; Pearlstone et al., 1992).

F29W/N domain (12–87) was constructed by the polymerase chain reaction using two 35-mer oligonucleotides and the *Eco*RI–*Sal*I fragment of pTZ18.NHdel/F29W as template. This latter construct was prepared initially in M13mp19.cIIFx.TnC (Golosinska et al., 1991) by site-specific mutagenesis to obtain a TnC clone in which amino acid residues 1–11 were deleted to obtain NHdel TnC. The replacement of F29 by W in NHdel TnC was achieved by site-specific mutagenesis using a pTZ18.NHdel TnC construct to obtain pTZ18.NHdel/F29W TnC. Details of the construction of these mutants will be described elsewhere (manuscript in preparation). The 5′-end oligonucleotide for the polymerase chain reaction was designed to include codons corresponding to amino acid residues 12–18 of TnC (underlined) flanked on the 5′ direction by nucleotides of the pET3a vector (Studier et al., 1990) including the *Nde*I restriction enzyme site:

5′-GAGATATACATATGGCCTTCCTCAGCGAG-GAGATG-3′.

The 3′ oligonucleotide includes a sequence (underlined) corresponding to amino acid residues 81–87 of the noncoding strand of the TnC gene. This is preceded in the 5′ direction by a complementary sequence for a stop codon (asterisk) and a *Bam*HI restiction site: 5′-CCCTTGGATCCCT*A-TTTCATCTGGCGCACCATCAT-3′. Polymerase chain reaction was performed in a Perkin Elmer thermal cycler (Model 480) using Taq polymerase and conditions essentially as described by Ho et al. (1989). The amplified DNA fragment was digested with the restriction enzymes *Nde*I–*Bam*HI and ligated into the *Nde*I–*Bam*HI sites of expression vector pET3a plasmid DNA (Studier et al., 1990). The ligation mixture was transformed into competent *E. coli* BL21 (DE3) pLys S cells and the entire region of the TnC gene was sequenced to ascertain the correctness of the amplification by the Taq polymerase enzyme. The expression of F29W/N-domain (12–87) TnC was carried out utilizing the isopropyl β-D-thiogalactopyranoside induction protocol (Studier et al., 1990). Cells from four 1-L cultures were resuspended in 50 mM Tris·HCl, pH 7.5, 1 mM EDTA, 25% sucrose, and 0.5 mM phenylmethanesulfonyl fluoride, the crude TnC was extracted by passing through a French press at 10 000 psi, and the cell debris was subsequently removed by centrifugation. To the supernatant were added $MgCl_2$, $CaCl_2$, NaCl, and DTT to a final concentration of 1 mM, 5 mM, 50 mM, and 1 mM, respectively. This was then directly applied to a phenyl-Sepharose CL-4B (Pharmacia) column and the separation of TnC carried out as described by Xu et al. (1991). Further purification was on DEAE-Sephadex A-25 essentially as described by Golosinska et al. (1991) for the purification of factor Xa-cleaved rTnC.

Spectral Measurements. Preparation of buffers and protein solutions was as before with appropriate precautions for the prevention of oxidation and contamination with Ca^{2+}. Calculation of free [Ca^{2+}], far-UV CD analyses, fluorescence measurements, protein concentration determinations, and curve-fitting of the Ca^{2+} titration data were described previously (Golosinska et al., 1991; Pearlstone et al., 1992). For all measurements, the buffer composition was 50 mM 3-(4-morpholino)propanesulfonic acid, pH 7.1, 100 mM KCl, and 1 mM EGTA with addition of appropriate amounts of 50 or 100 mM $CaCl_2$ to give the required pCa (where pCa = –log $[Ca]_{free}$).

Molecular Weight Determinations of F29W/N Domain (12–87) in the Presence and Absence of Ca^{2+}. These were carried out in the same buffer as above either with no addition of Ca^{2+} or at a pCa of 3.8. Instrumentation was a Beckman Model E analytical ultracentrifuge equipped with a photoelectric scanning absorbance optical system and titanium rotor. The conventional low-speed sedimentation equilibrium technique described by Chervenka (1970) was used for all runs. Protein samples (100 μL; 0.6–0.65 mg/mL) prepared as for the spectral measurements were loaded into 12-mm double-sector charcoal-filled Epon cells equipped with sapphire windows. Runs were at 20 °C for 48 h before equilibrium measurements were made. Rotor speeds were 28 000 and 32 000 rpm for plus and minus Ca^{2+} conditions, respectively. An assumed value of 0.728 was used for the partial specific volume (Byers & Kay, 1982). Molecular weight calculations were with a computer program written in APL language. The ln y versus r^2 data (where y is the fringe displacement and r is the distance from the axis of rotation in centimeters) were fitted to a second degree polynomial equation using least-squares techniques, and the weight average molecular weight was calculated from the slope of the resulting plot.

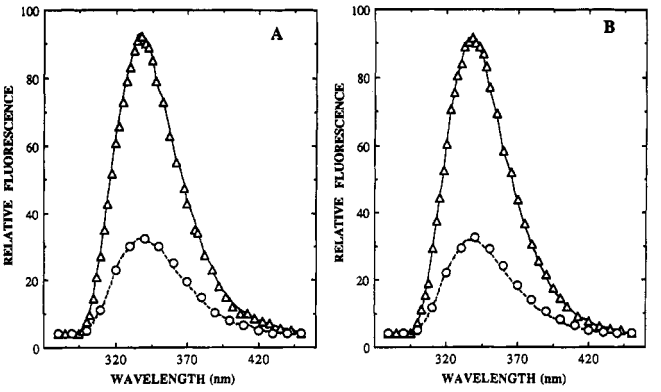

FIGURE 1: Fluorescence emission spectra of (A) F29W and (B) F29W/N domain (1–90). Buffer conditions were 50 mM 3-(*N*-morpholino)propanesulfonic acid, pH 7.1, 100 mM KCl, and 1 mM EGTA; 20 °C; protein concentration was 5 μM. Spectra were recorded in the presence of buffer only (- - -), 2 mM $CaCl_2$ (—), 44 mM $MgCl_2$ (○), or 2 mM $CaCl_2$ + 44 mM $MgCl_2$ (△). Excitation was at 282 nm.

Table 1: Quantum Yields of F29W and F105W Mutants in Different Ionic Conditions[a]

protein	minus Ca^{2+}	plus Ca^{2+}	plus Mg^{2+}	plus Ca^{2+}+Mg^{2+}
F29W	0.12	0.33	0.12	0.33
F29W/N domain (1–90)	0.12	0.33	0.12	0.33
F29W/N domain (12–87)	0.08	0.22	0.08	0.22
F105W	0.13	0.14	0.18	0.13
F105W/C domain (88–162)	0.13	0.16	0.20	0.16

[a] Buffer conditions were as described under Experimental Procedures. Ca^{2+} and Mg^{2+} concentrations, when present, were 2 and 44 mM, respectively.

RESULTS

Fluorescent Properties of F29W, F29W/N Domain (1–90), F105W, and F105W/C Domain (88–162). The fluorescent emission spectra of F29W and F29W/N domain (1–90) are shown in Figure 1A and Figure 1B, respectively. The spectra for the two are seen to be identical under all conditions. The excitation maxima were at 282 nm and emission maxima at 336 nm in both apo and Ca^{2+} states. The relative fluorescence intensity increased about 3-fold in going from the apo state (pCa = 8) to the Ca^{2+} state (pCa = 4). Using a quantum yield of 0.13 for free Trp as a standard in the same buffer (Eisinger, 1969), the quantum yield increased from 0.12 (apo) to 0.33 (+Ca^{2+}) in both cases (Table 1). There was no observed fluorescence change when 44 mM Mg^{2+} was added to the apo form of either protein. Titrations of the Ca^{2+}-induced fluorescence change as a function of free [Ca^{2+}] were also found to be identical for the two proteins (Figure 3). The monophasic curves were virtually superimposable and provided values for –log K_2 (Table 2) in good agreement with those previously reported for F29W (Pearlstone et al., 1992).

The Trp fluorescence emission spectra of F105W and F105W/C domain (88–162) in the absence and presence of divalent cations are shown in Figure 2A and Figure 2B, respectively. The spectra for the apo states of the two proteins are similar. Addition of Mg^{2+} to 44 mM led to a shift in the emission maximum from 343 nm (apo state) to 338 nm and a ~1.5-fold increase in fluorescence intensity, the same for both proteins. Addition of 2 mM $CaCl_2$ to F105W produced

Table 2: Ca^{2+} Binding Affinities for Intact rTnC Mutants and Its Isolated Domains

protein	low-affinity sites $-\log K_2$	high-affinity sites $-\log K_1$
F29W[a]	5.74 (±0.01)[b]	6.66 (±0.09)[b]
	5.73 (±0.01)[c]	
F29W/N domain (1–90)	5.80 (±0.03)[b]	
	5.65 (±0.02)[c]	
F105W		6.66 (±0.01)[c]
F105W/C domain (88–162)		6.93 (±0.01)[c]
C domain (88–162)		6.81 (±0.06)[b]
1:1 mix of F29W/N domain (1–90) plus C domain (88–162)	5.76 (±0.03)[b]	6.80 (±0.01)[b]
theoretical summation of F29W/N domain (1–90) plus C domain (88–162)	5.75[d]	6.83[d]

[a] Data taken from Pearlstone et al. (1992). [b] Ca^{2+} titrations of $[\theta]_{221nm}$; data sets from each of three to four titrations were analyzed as described by Golosinska et al. (1991) and Pearlstone et al. (1992) to give $-\log K$ values where K is the apparent dissociation constant. [c] Ca^{2+} titrations of fluorescence change; data sets for three titrations were analyzed as for the $[\theta]_{221nm}$ titrations. [d] These values were obtained by summation of the averaged curves and attributing 27% of the total ellipticity change to the N domain and 73% to the C domain.

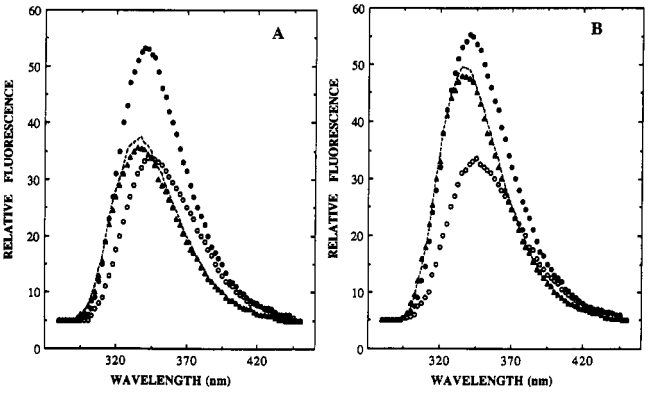

FIGURE 2: Fluorescence emission spectra of (A) F105W and (B) F105W/C domain (88–162). Buffer conditions as in Figure 1; buffer only (○); 2 mM $CaCl_2$ (- - -); 44 mM $MgCl_2$ (●); 2 mM $CaCl_2$ + 44 mM $MgCl_2$ (△). Protein concentration was 5 μM. Excitation was at 282 nm at 20 °C.

a small increase in fluorescence intensity and a shift in λ_{max} to 335 nm. With F105W/C domain (88–162), the increase in fluorescence at λ_{max} = 335 nm produced by addition of 2 mM Ca^{2+} was considerably larger. For both proteins, the addition of Ca^{2+} at 2 mM largely displaces Mg^{2+} at 44 mM. When the divalent cation-induced fluorescence change at 335 nm was monitored as a function of pCa, monophasic titration curves for both proteins were obtained (see Figure 3). That for F105W/C domain (88–162) was shifted moderately to higher pCa values, i.e., to lower free [Ca^{2+}]. Analysis of these curves provided $-\log K_1$ values of 6.66 and 6.93 for F105W and F105W/C domain (88–162), respectively (Table 2), indicating an approximately 2-fold increase in Ca^{2+} affinity for sites III/IV in the isolated C domain as compared with that for the same sites in the intact protein.

Comparison of Far-UV CD Properties of Isolated N and C Domains with Intact TnC. The far-UV CD spectra of F29W/N domain (1–90) and C domain (88–162) in the absence and presence of Ca^{2+} are shown in Figure 4A and Figure 4B, respectively. The corresponding $[\theta]_{221nm}$ values are given in Table 3. In agreement with previous studies [reviewed by Leavis and Gergely (1984)], Ca^{2+} binding to C domain (88–162) induces large increases in the negative ellipticity. The $[\theta]_{221nm}$ value in the apo state is seen to decrease

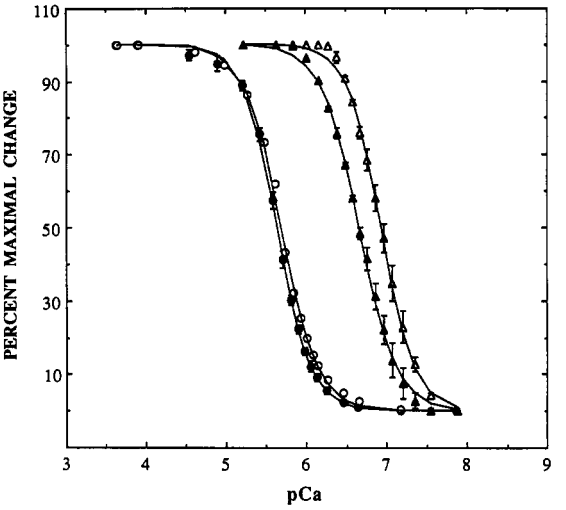

FIGURE 3: Ca^{2+} titration of the fluorescence change of F29W (○), F29W/N domain (1–90) (●), F105W (▲), and F105W/C domain (88–162) (△). Fluorescence excitation was at 282 nm, and emission was monitored at 336 nm for the F29W mutants and at 323 nm for the F105W proteins. Protein concentration was 5 μM, and the buffer was as in Figure 1; 20 °C. For each mutant, the average values for three or four titrations are shown by symbols with standard deviations as vertical bars. The fitted curves to the averaged data are shown by the solid lines.

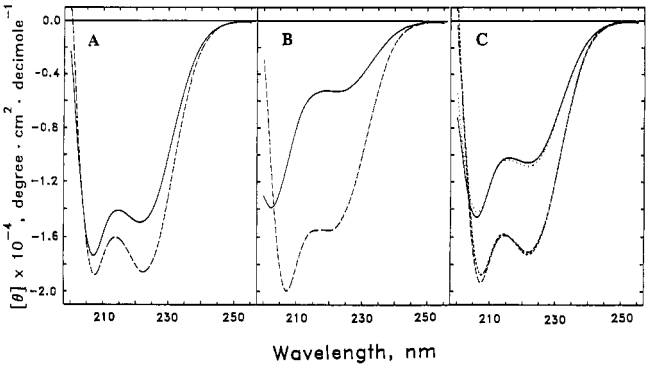

FIGURE 4: Far-UV CD spectra of (A) F29W/N domain (1–90): minus Ca^{2+} (—); plus Ca^{2+} (- - -). (B) C domain (88–162): minus Ca^{2+} (—); plus Ca^{2+} (- -). (C) Comparison of F29W with theoretical summation of (A) plus (B). F29W, minus Ca^{2+} (···), plus Ca^{2+} (- - -); (A) plus (B), minus Ca^{2+} (—), plus Ca^{2+} (– –). Buffer conditions were as in Figure 1 either with no $CaCl_2$ added (minus Ca^{2+}) or with addition to pCa 3.8 (plus Ca^{2+}). Protein concentrations were 30 μM at 25 °C. The summed spectra were calculated on the basis of the number of residues in each polypeptide chain (see footnote *c* of Table 3).

from −4980 ± 170 to −16 030 ± 520 deg·cm²·dmol⁻¹ upon addition of Ca^{2+} to pCa of 3.8. This has previously been interpreted in terms of a Ca^{2+}-induced conformational transition from a low level of preformed α-helical content in the apo form to a much more structured state in the Ca^{2+}-bound state, the latter presumably similar to that seen in the X-ray structure of the $2Ca^{2+}$ state of intact TnC. Surprisingly, on the other hand, and in contrast to previous reports (Nagy & Gergely, 1979; Leavis et al., 1978), we observe a smaller but very significant increase in negative ellipticity upon Ca^{2+} binding to isolated F29W/N domain (1–90). Averaged values of $[\theta]_{221nm}$ decrease from −15 390 ± 650 deg·cm²·dmol⁻¹ in the absence of Ca^{2+} to −18 910 ± 600 deg·cm²·dmol⁻¹ in its presence.

A theoretical summation of the spectra of Figure 4A,B for the isolated N and C domains was calculated and compared with intact F29W in Figure 4C. The summed and experimental spectra are seen to be virtually superimposable in both

Table 3: Far-UV Circular Dichroism Ellipticities (deg·cm²·dmol⁻¹) of Intact F29W and Its Isolated N and C Domains[a]

protein	$[\theta]_{221nm}$ minus Ca^{2+}	$[\theta]_{221nm}$ plus Ca^{2+}
F29W[b]	−10530 (±310)	−17490 (±590)
F29W/N domain (1–90)	−15390 (±650)	−18910 (±600)
F29W/N domain (12–87)	−15750 (±250)	−20520 (±400)
C domain (88–162)	−4980 (±170)	−16030 (±520)
theoretical summation of F29W/N domain (1–90) plus C domain (88–162)[c]	−10870 (±440)	−17930 (±570)
1:1 mix of F29W/N domain (1–90) plus C domain (88–162)	−10370 (±210)	−17100 (±300)

[a] Each value is the average of three to four determinations. [b] Data taken from Pearlstone et al. (1992). [c] The summation is based on the number of amino acid residues in each protein: 91 for F29W/N domain (1–90); 75 in C domain (88–162); 163 in F29W.

the apo and plus Ca^{2+} states. Corresponding values of $[\theta]_{221nm}$ for F29W, F29W/N domain (1–90), C domain (88–162), and a 1:1 molar mixture of the two domains as well as summed values for the two isolated domains are given in Table 3. The excellent agreement of the summed, 1:1 mixture, and intact F29W values in both minus and plus Ca^{2+} conditions indicates that the secondary structural features of the isolated N and C domains are very similar to those in the intact molecule. Because of the quality and good reproducibility of the data as well as the excellent agreement between the summed values for the two domains and those of the intact molecule, one can calculate the relative contributions of the two domains to the total Ca^{2+}-induced ellipticity change of the intact molecule. These were found to be 27% for the N domain and 73% for the C domain. The data also indicate that there is little effect of one domain on the other, either as a mixture of the two isolated domains or in the intact molecule, at least as assessed by these criteria.

Calcium titration curves of $[\theta]_{221nm}$ for F29W/N domain (1–90) and C domain (88–162) are shown in Figure 5A. For each set of averaged titration data, a monophasic curve could be fitted from which $-\log K_2$ and $-\log K_1$ values could be calculated (see Table 2). These values are seen to be in reasonable agreement with those obtained from Ca^{2+} titrations of the fluorescence emission of F29W/N domain (1–90) and of F105W/C domain (88–162). In Figure 5B, the $[\theta]_{221nm}$ *vs* pCa curves for each of the two domains of Figure 5A have been summed on the assumption that 73% of the total Ca^{2+}-induced ellipticity change has been contributed by the isolated C domain and 27% by the isolated N domain. This summed theoretical curve is compared with a titration curve of a 1:1 molar mixture of the two isolated domains and with that of intact F29W. Derived $-\log K_1$ and $-\log K_2$ values from each of these curves are given in Table 2. Those for $-\log K_2$ are seen to be the same within experimental error as those derived from the Ca^{2+} titration of the fluorescence emission of F29W/N domain (1–90) and of F29W. Similarly, the $-\log K_1$ values are in agreement with those calculated from fluorescence titration of F105W/C domain (88–162). The data reinforce the earlier conclusion that while the Ca^{2+} affinities of the isolated N-domain sites I and II are indistinguishable from those of the intact TnC molecule, those of sites III/IV of the isolated C domain are moderately increased by a factor of ~2. The Ca^{2+} affinities of each of the isolated domains are not affected by the presence of the other domain in a 1:1 mixture.

Spectral and Ca^{2+} Binding Properties of F29W/N Domain (12–87). The Ca^{2+}-induced changes in fluorescence and

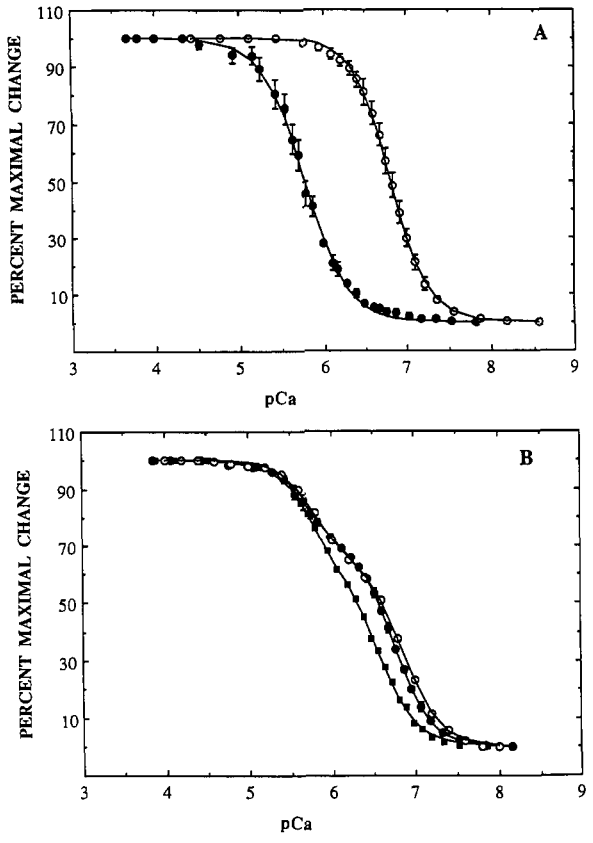

FIGURE 5: Ca^{2+} titration of far-UV CD $[\theta]_{221nm}$ of (A) F29W/N domain (1–90) (●) and C domain (88–162) (○), (B) F29W (■): 1:1 mixture of F29W/N domain (1–90) and C domain (88–162) (●) and theoretical summation of F29W/N domain (1–90) and C domain (88–162) assuming 27% and 73% contrib utions to the total $[\theta]_{221nm}$ change, respectively (○). Buffer conditions were as in Figure 1; protein concentration was 30 μM at 25 °C. Data points are averages of three or more titrations with standard deviations shown as vertical bars. The fitted curves to the averaged data points are shown by solid lines.

ellipticity described above for isolated F29W/N domain (1–90) are clearly indicative of a substantial conformational transition in the regulatory domain of TnC. These observed spectral changes are surprising in light of a previous report (Leavis et al., 1978) that tryptic fragment TR1C of rabbit skeletal muscle TnC (residues 9–84; rabbit protein numbering) shows no such Ca^{2+}-induced spectral changes. To further investigate this apparent discrepancy, we have engineered a truncated version of the chicken N domain [F29W/N domain (12–87)] which corresponds exactly to those residues of the rabbit TR1C fragment (residues 9–84; rabbit protein numbering). This truncated version of the N domain is largely lacking the N helix (residues 3–13 in the crystal structures of the avian proteins) and is shortened by three residues (88–90) in the D/E helix.

The far-UV CD spectra and the fluorescence emission spectra of F29W/N domain (12–87) in the presence and absence of Ca^{2+} are shown in Figures 6 and 7, respectively. The corresponding $[\theta]_{221nm}$ values are listed in Table 3. These are seen to be similar to but not identical to those observed for F29W/N domain (1–90). While the $[\theta]_{221nm}$ values for F29W/N domain (12–87) and F29W/N domain (1–90) in the absence of Ca^{2+} are the same within experimental error, the value for F29W/N domain (12–87) in the presence of Ca^{2+} is significantly higher than that for F29W/N domain (1–90). Similarly, the fluorescence emission spectra of the truncated and intact N-domain preparations are similar but not identical (compare quantum yields in Table 1 in $\pm Ca^{2+}$/

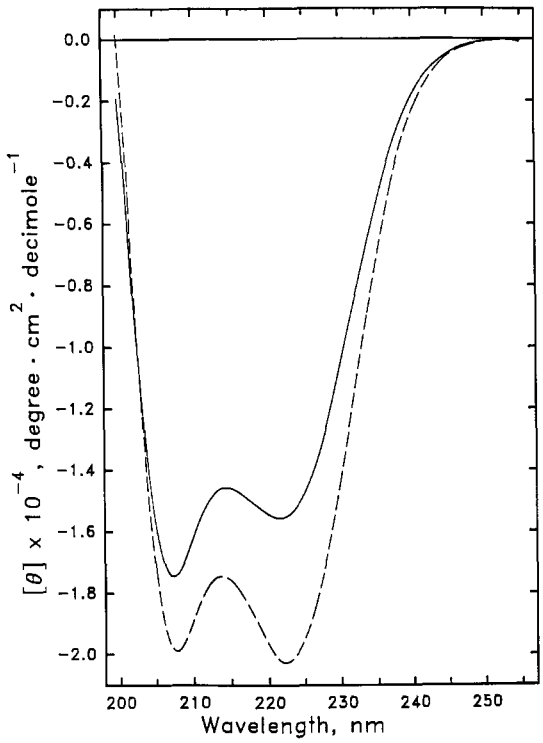

FIGURE 6: Far-UV CD spectra of F29W/N domain (12–87) in the absence (—) and presenc of Ca^{2+} (pCa = 3.8) (– –). Buffer conditions were as in Figure 1. Protein concentration was 30 μM at 25 °C. Each spectrum represents the average of three or four experiments.

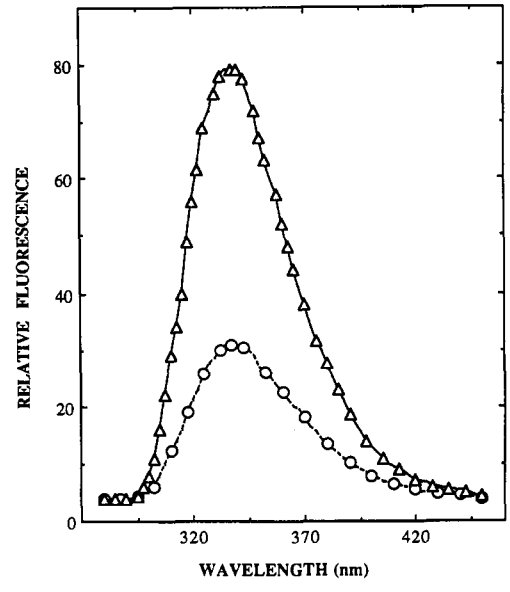

FIGURE 7: Emission fluorescence spectra of F29W/N domain (12–87) in the absence of Ca^{2+} (- - -) and in the presence of 2 mM $CaCl_2$ (—), 44 mM $MgCl_2$ (○), and 2 mM $CaCl_2$ + 44 mM $MgCl_2$ (△). Protein concentration was 5 μM at 20 °C. Buffer conditions were as in Figure 1. Excitation was at 282 nm.

Mg^{2+} conditions). In spite of the differences between F29W/N domain (1–90) and F29W/N domain (12–87), it is clear that the truncated version does undergo a substantial Ca^{2+}-induced structural transition. When the fluorescence emission and $[\theta]_{221nm}$ of F29W/N domain (12–87) were monitored as a function of free $[Ca^{2+}]$, i.e., pCa^{2+}, the agreement between the two titration curves and in the derived $-\log K_2$ values was poor (data not shown). Since the protein concentrations in these two types of measurements are different, the effects of protein concentration on the fluorescence titration curves were examined. Figure 8A shows that

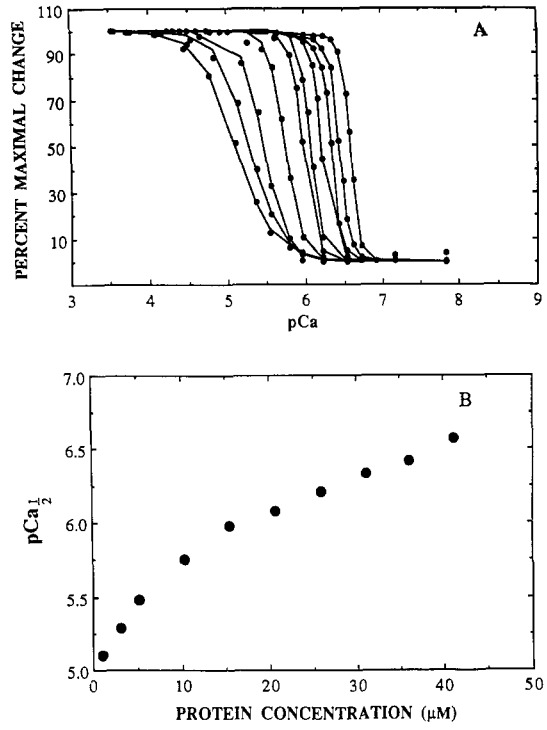

FIGURE 8: Effects of protein concentration on the Ca^{2+} affinity of F29W/N domain (12–87). (A) Ca^{2+} titrations of the emission fluorescence change at increasing protein concentrations from left to right: 1, 3, 5, 10, 15, 20, 25, 30, 35, and 40 μM. Buffer conditions as in Figure 1; 20 °C. Excitation was at 282 nm, and emission was monitored at 336 nm. (B) Relationship between $pCa_{1/2}$ values from panel A and protein concentration.

as the concentration of F29W/N domain (12–87) is increased, the pCa versus relative fluorescence curves are markedly shifted to lower $[Ca^{2+}]$, indicative of a markedly increased Ca^{2+} affinity. A concomitant increase in the slope of these curves is also observed. Figure 8B illustrates the increase in $pCa_{1/2}$ as a function of concentration of the truncated fragment. The $pCa_{1/2}$ increases from 5.3 to 7.0 as the protein concentration is increased from 1 to 40 μM. In control experiments, no such concentration dependence was observed for either intact F29W or F29W/N domain (1–90). Since such an effect could be associated with a Ca^{2+}-dependent aggregation of the truncated fragment, we have examined the weight average molecular weight of F29W/N domain (12–87) both in the absence and in the presence of Ca^{2+}. In the absence of Ca^{2+}, the linearity of the plot of ln y versus r^2 and the calculated molecular weight value of 8790 ± 115 (average of three determinations) are consistent with a totally monomeric form of the fragment in solution. When Ca^{2+} is present, the plot of ln y versus r^2 showed upward curvature with an average molecular weight value of 11 370 ± 1290 (average of three determinations), indicating a mixture of monomeric, dimeric, and perhaps polymeric forms in solution. These data are certainly consistent with an interpretation of the protein concentration dependence of the titration data as arising from Ca^{2+}-induced aggregation, an effect that is clearly more evident with the truncated fragment than with intact TnC or with F29W/N domain (1–90).

DISCUSSION

In previous studies (Pearlstone et al., 1992; Trigo-Gonzalez et al., 1992), we have shown that appropriate mutations of Phe to Trp residues in recombinant chicken TnC can serve as useful reporter groups for monitoring divalent metal cation-

induced conformational transitions in the N and C domains of this protein. Since the chicken protein is naturally devoid of Tyr and Trp residues, spectral features can be unambiguously assigned to the mutated residues. Characterization of these mutants, F29W in the N domain and F105W in the C domain, has shown them to be specific for their respective domains and not to be significantly influenced by metal-induced conformational events in the other domain. Since a number of other studies [reviewed by Grabarek et al., (1992)] have provided evidence for some degree of interdomain interactions, we have, in the present work, compared the properties of isolated engineered N and C domains, each carrying a Phe → Trp mutant, with intact TnCs, also bearing the appropriate Trp mutants. On the basis of the crystallographic structure, chain termination (residue 90) and initiation (residue 88) sites for the preparation of the isolated domains were chosen such that there would be minimal disruption of side-chain interactions between D/E helical residues and those of their respective domains. A further consideration was that the polypeptide chain in the region of Cys-101 is considered to be a putative binding site for the inhibitory region of TnI. These choices were considered to be advantageous over previous studies which were dependent on fragments generated by either proteolytic or chemical degradation at available cleavage sites. In particular, the TR1C fragment (residues 9–84 of rabbit TnC) lacks residues 1–8 comprising a major portion of the N helix in the crystallographic structure. Similarly, chemical cleavage at Cys-101 (Swenson & Fredricksen, 1992) is expected to have a destabilizing effect on the C domain as well as to adversely affect potential interaction studies with TnI and its fragments. It was also considered that the use of Phe → Trp mutants as spectral probes for monitoring conformational transitions rather than the introduction by chemical derivatization of large aromatic fluorescent probes would be advantageous in more closely reflecting the properties of the native molecule.

The far-UV CD studies of the two isolated domains reported herein indicate that the overall secondary structural features of the two domains are the same whether free in solution or as part of the intact molecule. Comparison of the summed spectra and $[\theta]_{221nm}$ values of the two domains shows them to be virtually identical with those of the intact molecule and the same as a 1:1 mixture of the two isolated domains (see Figure 4 and Table 3). This was true both in the absence as well as in the presence of Ca^{2+}.

In the case of F29W/N domain (1–90), the fluorescence and Ca^{2+} binding properties were also found to be identical to those for intact F29W. Thus, both the emission spectra and quantum yields of the two proteins were the same in both the apo and Ca^{2+}-loaded states. Addition of $MgCl_2$ to 44 mM had no effect on the fluorescence emission spectrum of either protein preparation. Titration of the Ca^{2+}-induced fluorescence increase as a function of pCa gave values of the apparent dissociation constants, K_2, which were identical (see Figure 3 and Table 2). These were also in good agreement with the K_2 values derived from the $[\theta]_{221nm}$ versus pCa curves of F29W/N domain (1–90) and intact F29W (see Table 2). By all these criteria then, we observe no differences in the properties of the isolated N domain and those of the N domain in the intact protein.

The spectral and metal binding properties of F105W/C domain (88–162) and intact F105W, on the other hand, were found to be very similar but not identical. Although the fluorescence spectra and quantum yields of the C domain and intact protein in the apo state were the same, those in the Ca^{2+}- and Mg^{2+}-loaded states showed small but significant differences. Ca^{2+} titration of the induced fluorescence changes also demonstrated a small increase in Ca^{2+} affinity attributable to sites III/IV of the isolated C domain (see Figure 3 and Table 2). This increase in Ca^{2+} affinity was also seen in the $[\theta]_{221nm}$ versus pCa^{2+} titration curves of C domain (88–162) when compared with the intact protein (see Figure 5 and Table 2). This increase in Ca^{2+} affinity of the isolated C domain is similar to that previously observed with the analogous tryptic fragment TR2C encompassing residues 89–159 of rabbit skeletal muscle TnC (Leavis et al., 1978).

As detailed above, we observe a significant Ca^{2+}-induced conformational transition in N domain (1–90) as monitored by both fluorescence and far-UV CD. Since a previous study (Leavis et al., 1978) reported no such Ca^{2+}-induced transition in the tryptic fragment TR1C (residues 9–84 of rabbit skeletal TnC), we have engineered and expressed the corresponding truncated N-terminal fragment F29W/N domain (12–87) of the chicken gene. As with the intact F29W/N domain (1–90), significant Ca^{2+}-induced fluorescence and negative ellipticity transitions were observed. These were similar although not identical to those seen in the present work with intact F29W and F29W/N domain (1–90). We must conclude that the earlier failure to detect such Ca^{2+}-induced ellipticity changes with rabbit TR1C was probably a reflection of less adequate instrumentation which, in the interim, has been very significantly improved.

In the present study, we have observed a very significant protein concentration dependence of the Ca^{2+}-induced conformational transition of F29W/N domain (12–87) not seen either with intact F29W or with F29W/N domain (1–90). We have attributed this concentration dependence to Ca^{2+}-induced aggregation of the truncated fragment since molecular weight measurements gave values corresponding to the monomeric form in the absence of Ca^{2+} and to higher molecular weight forms upon addition of Ca^{2+}. Although native intact TnC is known to undergo Ca^{2+}-induced dimerization (Margossian & Stafford, 1982; Fujisawa et al., 1990), this phenomenon is clearly much more extensive with truncated N domain (12–87) than with the intact protein or with N domain (1–90) since these do not show this concentration dependence. Inspection of the crystal structure of avian TnC (Herzberg & James, 1985a,b, 1988; Satyshur et al., 1988; Sundaralingam et al., 1985) reveals that residues 1–11 constitute a significant portion of helix N of the intact protein. In the known $2Ca^{2+}$ and postulated $4Ca^{2+}$ states of the protein (Herzberg et al., 1986), helix N makes multiple side-chain contacts with both helices A and D involving a number of hydrophobic side chains in all three helices. Assuming no gross changes in the relative disposition of secondary structural elements, the removal of residues 1–11 would lead to the surface exposure of a number of nonpolar side-chain residues in both helix A and helix D. Their exposure, however, does not lead to aggregation in the apo state but does in the $2Ca^{2+}$ state. Thus, the phenomenon must involve Ca^{2+}-induced alterations in surface topology, probably in addition to those involving the exposed nonpolar residues of helices A and D resulting from deletion of residues 1–11. Obvious candidates are those residues believed to become more exposed to form the "hydrophobic patch" in the transition to the Ca^{2+}-saturated state of the regulatory domain (Herzberg et al., 1986).

Recently a preliminary NMR structure of the apo form of the TR1C fragment of turkey skeletal TnC has been reported (Findlay & Sykes, 1993). Its secondary structural features and global fold were found to be very similar to those of the

corresponding region of the crystallographic structure of whole TnC, although some apparent differences in the A and B helices were noted. The present data on the engineered chicken skeletal muscle truncated N domain (12–87), which is identical in amino acid sequence to that of turkey TR1C (Golosinska et al., 1991), also indicate that the structural features of this fragment are rather similar, but not identical, to N domain (1–90) and to the N domain in intact TnC. These nonidentities were observed both in the apo state and also in the Ca^{2+}-saturated state, and suggest that the Ca^{2+}-induced structural transition of TR1C is not fully representative of that occurring in the N domain of intact TnC. The data also indicate that removal of residues 1–11, i.e., the N helix, has to some degree affected the structure and properties of the N domain. The truncation (residues 88–90) of TR1C at its COOH-terminal end when compared with N domain (1–90) may also affect its structure and properties. These structural differences, although modest, may be of critical importance in the N domain's functional role in Ca^{2+} regulation of the muscle thin filament system.

The Ca^{2+}-induced structural transition of the N domain of TnC is believed to be the key event in the Ca^{2+} regulation of muscle contraction and relaxation. Compared with the large changes in ellipticity and other spectral features observed by Ca^{2+} binding to C-domain sites III/IV [see review by Leavis and Gergely (1984)], those attributed to N-domain sites I/II are more subtle, less clearly defined, and to some degree contradictory. On the basis of their far-UV CD studies with intact rabbit skeletal muscle TnC, Nagy and Gergely (1979) concluded that the small (~10%) Ca^{2+}-induced far-UV CD changes could be accounted for by a small increase in α-helical content involving perhaps only the addition of a peptide unit of two to one or more of the preexisting α-helical segments in the N-domain half of the molecule. This view appeared to be reinforced by the apparent absence of Ca^{2+}-induced far-UV CD changes in the isolated TR1C fragment (residues 9–84) of the rabbit protein (Leavis et al., 1978) and by several early spectral, laser Raman spectroscopic, and proton NMR studies on intact TnC (Levine et al., 1977, 1978; Seamon et al., 1977; Leavis et al., 1980; Carew et al., 1980; Evans et al., 1980). These latter measurements with intact TnC, however, were against a high background of divalent metal ion-induced changes attributable to the C domain and in the case of the NMR data involved only the assignment of a few resonances. Two other reports, however (Johnson & Potter, 1978; Hincke et al., 1978), have reported a much larger (30–40%) Ca^{2+}-evoked increase in the far-UV negative ellipticity associated with the filling of N-domain sites I/II. The observations reported in the present paper are clearly in much better agreement with the latter two reports. These demonstrate that summation of the Ca^{2+}-induced ellipticity change in the two isolated domains is in excellent agreement with the total negative ellipticity change observed for the intact molecule (see Figure 4 and Table 3) and that of this total ~73% can be attributed to the C domain and ~27% to the N domain. This appreciable Ca^{2+}-induced increase in negative ellipticity of the N domain suggests a significant change in secondary structure. Using the method of Provencher and Glöckner (1981), it can be calculated that the apparent α-helical content of the N domain would increase from 47% to 61%, corresponding to an incorporation into α-helices of 12–13 peptide residues. Although the interpretation of ellipticity changes in terms of such numbers is fraught with uncertainties, the present observations strongly suggest that the Ca^{2+}-evoked secondary structural changes in the N domain are more substantial than has been previously appreciated.

Recent developments in NMR technology now permit the determination of protein structures the size of troponin C and calmodulin (Ikura et al., 1992) in solution at physiological pH. The present demonstration that the properties of the isolated N domain (1–90) of rTnC closely reflect those of this domain in the intact molecule indicates its potential for elucidation of the important Ca^{2+}-induced structural transitions of this regulatory element in muscle contraction, a project currently in progress in our laboratories.

ACKNOWLEDGMENT

We are indebted to Dr. M. N. G. James for his advice in the design of mutants and to Dr. W. D. McCubbin for helpful discussions. We thank Mrs. Linda Weiner and Mr. Pierre Dubord for their assistance in the purification of proteins and for amino acid analyses, Mr. Kim Oikawa for the circular dichroism measurements, and Mr. Leslie D. Hicks for the ultracentrifuge measurements.

REFERENCES

Byers, D. M., & Kay, C. M. (1982) *Biochemistry 21*, 229–233.
Carew, E. B., Leavis, P. C., Stanley, H. E., & Gergely, J. (1980) *Biophys. J. 30*, 351–358.
Carter, P., Bedouelle, H., & Winter, G. (1985) *Nucleic Acids Res. 13*, 4431–4443.
Chervenka, C. H. (1970) *A Manual of Methods for the Analytical Ultracentrifuge*, Spinco Division of Beckman Instruments, Palo Alto, CA.
Eisinger, J. (1969) *Photochem. Photobiol. 9*, 247–259.
Evans, J. S., Levine, B. A., Leavis, P. C., Gergely, J., Grabarek, Z., & Drabikowski, W. (1980) *Biochim. Biophys. Acta 623*, 10–20.
Findlay, W. A., & Sykes, B. D. (1993) *Biochemistry 32*, 3461–3467.
Fujisawa, T., Ueki, T., & Iida, S. (1990) *J. Biochem. 107*, 343–351.
Golosinska, K., Pearlstone, J. R., Borgford, T., Oikawa, K., Kay, C. M., Carpenter, M. R., & Smillie, L. B. (1991) *J. Biol. Chem. 266*, 15797–15809.
Grabarek, Z., Drabikowski, W., Leavis, P. C., Rosenfeld, S. S., & Gergely, J. (1981) *J. Biol. Chem. 256*, 13121–13127.
Grabarek, Z., Tao, T., & Gergely, J. (1992) *J. Muscle Res. Cell Motil. 13*, 383–393.
Grand, R. J. A. (1985) *Top. Mol. Struct. Biol. 7*, 65–122.
Herzberg, O., & James, M. N. G. (1985a) *Nature 313*, 653–659.
Herzberg, O., & James, M. N. G. (1985b) *Biochemistry 24*, 5298–5302.
Herzberg, O., & James, M. N. G. (1988) *J. Mol. Biol. 203*, 761–768.
Herzberg, O., Moult, J., & James, M. N. G. (1986) *J. Biol. Chem. 261*, 2638–2644.
Hincke, M. T., McCubbin, W. D., & Kay, C. M. (1978) *Can. J. Biochem. 56*, 384–395.
Ho, S. N., Hunt, H. D., Horton, R. M., Pullen, J. K., & Pease, L. R. (1989) *Gene 77*, 51–59.
Ikura, M., Clore, G. M., Gronenborn, A. M., Zhu, G., Klee, C. B., & Bax, A. (1992) *Science 256*, 632–638.
Johnson, J. D., & Potter, J. D. (1978) *J. Biol. Chem. 253*, 3775–3777.
Kunkel, A. T., Roberts, J. D., & Zakour, R. A. (1987) *Methods Enzymol. 154*, 367–382.
Leavis, P. C., & Gergely, J. (1984) *CRC Crit. Rev. Biochem. 16*, 235–305.
Leavis, P. C., Rosenfeld, S. S., Gergely, J., Grabarek, Z., & Drabikowski, W. (1978) *J. Biol. Chem. 253*, 5452–5457.
Leavis, P. C., Nagy, B., Lehrer, S. S., Bialkowsky, H., & Gergely, J. (1980) *Arch. Biochem. Biophys. 200*, 17–21.

Leavis, P. C., Evans, J. S., & Levine, B. A. (1982) *J. Inorg. Biochem. 16*, 257–277.
Levine, B. A., Mercola, D., Hoffman, D., & Thornton, J. M. (1977) *J. Mol. Biol. 115*, 743–760.
Levine, B. A., Thornton, J. M., Fernandes, R., Kelly, C. M., & Mercola, D. (1978) *Biochim. Biophys. Acta 535*, 11–24.
Margossian, S. S., & Stafford, W. F. (1982) *J. Biol. Chem. 257*, 1160–1165.
McCubbin, W. D., Oikawa, K., Sykes, B. D., & Kay, C. M. (1982) *Biochemistry 21*, 5948–5956.
Mead, D. A., Skorupa, E. S., & Kemper, B. (1986) *Protein Eng. 1*, 67–74.
Nagy, B., & Gergely, J. (1979) *J. Biol. Chem. 254*, 12732–12737.
Parmacek, M. S., & Leiden, J. M. (1991) *Circulation 84*, 991–1003.
Pearlstone, J. R., Borgford, T., Chandra, M., Oikawa, K., Kay, C. M., Herzberg, O., Moult, J., Herklotz, A., Reinach, F. C., & Smillie, L. B. (1992) *Biochemistry 31*, 6545–6553.
Potter, J. D., & Johnson, J. D. (1982) in *Calcium and Cell Function* (Cheung, W., Ed.) Vol. 2, pp 145–173, Academic Press, New York.
Provencher, S. W., & Glöckner, J. (1981) *Biochemistry 20*, 33–37.
Reinach, F. C., & Karlsson, R. (1988) *J. Biol. Chem. 263*, 2371–2376.
Satyshur, K. A., Rao, S. T., Pyzalska, D., Drendel, W., Greaser, M., & Sundaralingam, M. (1988) *J. Biol. Chem. 263*, 1628–1647.
Seamon, K. B., Hartshorne, D. J., & Bothner-By, A. A. (1977) *Biochemistry 16*, 4039–4046.
Strynadka, N. C. J., & James, M. N. G. (1989) *Annu. Rev. Biochem. 58*, 951–998.
Studier, F. W., Rosenberg, A. H., Dunn, J. J., & Dubenforff, J. W. (1990) *Methods Enzymol. 185*, 60–89.
Sundaralingam, M., Bergstrom, R., Strasburg, G., Rao, S. T., Roychowdhury, P., Greaser, M., & Wang, B. C. (1985) *Science 227*, 945–948.
Swenson, C. A., & Fredricksen, R. S. (1992) *Biochemistry 31*, 3420–3429.
Trigo-Gonzalez, G., Racher, K., Burtnick, L., & Borgford, T. (1992) *Biochemistry 31*, 7009–7015.
Xu, G. Q., & Hitchcock-DeGregori, S. E. (1988) *J. Biol. Chem. 263*, 13962–13969.
Zot, H. G., & Potter, J. D. (1987) *Annu. Rev. Biophys. Biophys. Chem. 16*, 535–559.